

100 mW deep-ultraviolet emission from aluminium-nitride-based quantum wells pumped by an electron beam

Takao Oto¹, Ryan G. Banal¹, Ken Kataoka², Mitsuru Funato¹ and Yoichi Kawakami^{1*}

Ultraviolet light sources, represented by excimer and mercury lamps, are currently used for various applications, including water purification/sterilization, biotechnology, photolithography and surface modification. However, they have the disadvantages of limited portability, low emission efficiency and the presence of harmful constituents. Finding a compact, efficient and environmentally friendly alternative ultraviolet light source is therefore of considerable technological interest. Aluminium-nitride-based semiconductors show promise as materials for this purpose^{1–13}, but because of difficulties in controlling electronic conductivity, in light-emitting diodes are hampered by low external quantum efficiencies. Here, we use an electron-beam pumping technique, demonstrating an output of 100 mW and a record power efficiency of ~40% from Al_xGa_{1–x}N/AlN quantum wells emitting at ~240 nm. This achievement is attributed to carrier confinement within the high-quality quantum wells, as well as the appropriate design of sample structures for electron-beam pumping, and may be a milestone in the path to realizing next-generation ultraviolet light sources with great ecological and economic benefits.

Aluminium nitride (AlN) and high-aluminium-content Al_xGa_{1–x}N/AlN quantum wells have recently been the subject of extensive study^{1–13}, because Al_xGa_{1–x}N has a direct bandgap that can be tuned for the ultraviolet (UV) region between 200 and 300 nm by adjusting the composition of the aluminium. Crystal quality has now been improved dramatically, enabling internal quantum efficiencies (IQEs) at room temperature to reach 70% (see Methods) at a wavelength of 280 nm (ref. 4) and 50% at 250 nm (ref. 5). We have also fabricated high-quality Al_xGa_{1–x}N/AlN quantum wells on sapphire (0001) substrates^{6–8} that have an IQE of 36% at 240 nm (ref. 8). These values are comparable to matured In_xGa_{1–x}N/GaN visible emitters¹⁴.

A critical factor in electrically driven devices such as light-emitting diodes (LEDs) is the external quantum efficiency (EQE), which is the product of the IQE, carrier injection efficiency (CIE) and light extraction efficiency (LEE). Despite the high IQE that has been achieved, the EQE of Al_xGa_{1–x}N-based LEDs is only ~3% for emissions between 255 and ~280 nm (refs 10,11) and becomes smaller at shorter wavelengths¹². Although their reported LEE values are less than 8% (ref. 13), device configurations such as patterned substrates¹⁵ may improve the LEE. A more essential factor responsible for a low EQE may be the intrinsically low hole concentrations in *p*-type Al_xGa_{1–x}N. Generally, the wider the bandgap, the deeper the acceptor activation energy becomes; this has been observed in magnesium-doped AlN (630 meV; ref. 1) and GaAs (29 meV; ref. 16). A simple calculation based on Maxwell–Boltzmann statistics predicts that the hole concentration in AlN with a magnesium

acceptor concentration of $1 \times 10^{19} \text{ cm}^{-3}$ is $\sim 2 \times 10^{10} \text{ cm}^{-3}$ at room temperature. This very low value degrades the hole-related transport properties.

Several groups have proposed a promising alternative—electron-beam (EB) pumped nitride semiconductor-based light sources—which use a structure similar to a field-emission display. Watanabe and colleagues have fabricated a handheld device using boron nitride powders with an emission wavelength of 225 nm, a maximum output power (P_{out}) of 1 mW, and a power efficiency (PE) of 0.6% (ref. 17). Additionally, Miyake and colleagues have demonstrated that a silicon-doped Al_xGa_{1–x}N bulk-like film excited by EB exhibits an output of 2.2 mW at 247 nm with a PE of 0.22% (ref. 18). However, similar to LEDs^{12,13}, their performances are still insufficient for practical applications.

There are two major reasons for this poor performance. The first arises from self-absorption phenomena, in that light-emitting bulks and powders may absorb emitted light, degrading its availability. (In LEDs, the *p*-type GaN used for improving hole transport properties also absorbs emitted light.) The second reason is that the radiative recombination probabilities in bulks and powders are low compared with quantum wells¹⁹. To overcome these issues, we propose using highly luminous quantum wells as a phosphor for EB pumping.

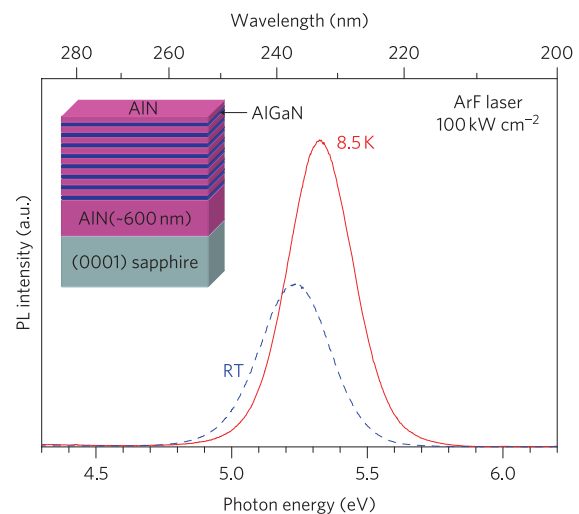


Figure 1 | Fundamental optical properties. The inset is a schematic of an Al_{0.69}Ga_{0.31}N/AlN MQW grown on AlN (600 nm)/sapphire (0001). PL spectra of Al_{0.69}Ga_{0.31}N/AlN MQW were acquired at 8.5 K and room temperature, from which the IQE was evaluated to be 57%.

¹Department of Electronic Science and Engineering, Kyoto University, Kyoto 615-8510, Japan, ²SSLS Development Department, Ushio Inc., Himeji, Hyogo 671-0224, Japan. *e-mail: kawakami@kuee.kyoto-u.ac.jp

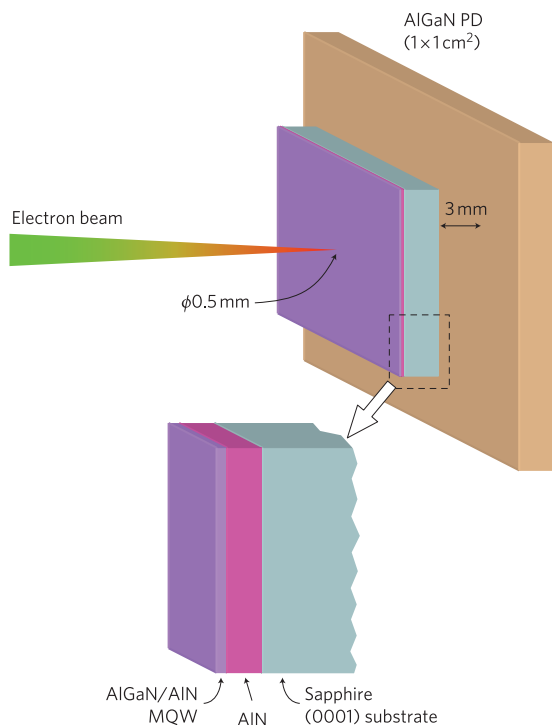


Figure 2 | Schematic configuration of EB pumping experiments.

$\text{Al}_{0.69}\text{Ga}_{0.31}\text{N}/\text{AlN}$ MQW with a rough back side is irradiated with a focused EB. An $\text{Al}_x\text{Ga}_{1-x}\text{N}$ photodiode is placed 3 mm behind the sample and monitors the emission power through the substrate.

In quantum wells, the light-emitting layer has a narrower bandgap than the host material, so absorption by the host material can be avoided in principle. Furthermore, as mentioned above, we have obtained $\text{Al}_x\text{Ga}_{1-x}\text{N}/\text{AlN}$ quantum wells with high IQEs. By virtue of these advantages, we now demonstrate a light output of 100 mW and a PE of $\sim 40\%$ at ~ 240 nm from $\text{Al}_x\text{Ga}_{1-x}\text{N}/\text{AlN}$ quantum wells pumped by EB.

As illustrated in the inset of Fig. 1, the sample comprised an $\text{Al}_x\text{Ga}_{1-x}\text{N}/\text{AlN}$ eight-period multiple quantum well (MQW) with an aluminium composition x of 0.69, grown on an $\text{AlN}/\text{sapphire}$ (0001) substrate (see Methods). The $\text{Al}_x\text{Ga}_{1-x}\text{N}$ well and AlN barrier thicknesses were 1 and 15 nm, respectively, yielding a 128-nm-thick quantum-well region. The reason for the selection of this thin well width is related to the optical anisotropy in $\text{Al}_x\text{Ga}_{1-x}\text{N}/\text{AlN}$ quantum wells⁹. In thick $\text{Al}_x\text{Ga}_{1-x}\text{N}$ coherently grown on AlN , the valence band ordering prevents surface emission from the (0001) plane for $x > 0.6$, that is, for emission wavelengths shorter than 250 nm. In contrast, we have found that the quantum confinement strongly affects the valence band ordering and promotes (0001) surface emission⁹, which motivated us to use the 1-nm-thick quantum well.

To assess the fundamental optical properties, photoluminescence (PL) measurements were performed at 8.5 K and room temperature (see Methods). Figure 1 shows the acquired PL spectra with an emission wavelength of ~ 237 nm at room temperature. The PL intensity ratio between room temperature and 8.5 K estimated the IQE at room temperature to be as high as 57%. It is noteworthy that the IQE of an AlN thick film has been estimated to be $\sim 5\%$ at room temperature³. The much higher IQE of our quantum well is due to the carrier confinement within the very high-quality quantum well. Before achieving this value, it was necessary to optimize the formation of the $\text{AlN}/\text{sapphire}$ interface⁶ and the crystal growth of AlN and $\text{Al}_x\text{Ga}_{1-x}\text{N}$ (refs 7,8). Another important finding in Fig. 1 is that emission from AlN is not observed, indicating that

carriers generated in the AlN barriers are eventually captured in the $\text{Al}_x\text{Ga}_{1-x}\text{N}$ wells. Thus, thin $\text{Al}_x\text{Ga}_{1-x}\text{N}$ wells (1 nm) and sufficiently thick AlN barriers (15 nm) are desirable in order to suppress self-absorption in the $\text{Al}_x\text{Ga}_{1-x}\text{N}$ wells and to supply them with as many carriers as possible.

Figure 2 schematically depicts the setup of the EB pumping experiments (see Methods). An EB was focused on the sample surface with a diameter of 0.5 mm. The photodetector, a $1 \times 1 \text{ cm}^2$ $\text{Al}_x\text{Ga}_{1-x}\text{N}$ photodiode, was placed 3 mm behind the sample to monitor the emission power through the sapphire substrate. To enhance light extraction by avoiding total reflection at the substrate/vacuum interface, the back of the substrate was roughened by a mechanical process. We confirmed that this roughened surface enhanced the light extraction by $\sim 50\%$.

Figure 3 presents the cathodoluminescence (CL) spectrum of the $\text{Al}_{0.69}\text{Ga}_{0.31}\text{N}/\text{AlN}$ MQW and the responsivity of the $\text{Al}_x\text{Ga}_{1-x}\text{N}$ photodiode. The band-edge emissions from AlN and $\text{Al}_{0.69}\text{Ga}_{0.31}\text{N}$ were observed at 210 and 238 nm, respectively. A relatively weak deep-level emission at ~ 320 nm was due to the $\text{AlN}/\text{sapphire}$ interface region, which was rich in mismatch dislocations, because that emission was detected though the substrate, but was not from the surface. Because the $\text{Al}_x\text{Ga}_{1-x}\text{N}$ photodiode was insensitive to light with wavelengths longer than 280 nm, only the emission near the band edge contributed to the estimation of P_{out} .

Electrons irradiated onto a solid penetrate into the solid and experience mutual interactions with other electrons and atomic nuclei. The penetration depths are generally larger for higher acceleration voltages (V_A) and lower-density solids. If the penetration depth is much greater than the thickness of the quantum well region, some of the irradiated electrons may go through that region and recombine in the underlying AlN layer, degrading the CIE. However, if the penetration depth is too narrow, then quantum wells located deeper away from the surface do not receive a sufficient number of carriers. Therefore, to maximize the PE and P_{out} , appropriately selecting V_A to match a given quantum well structure or, conversely, designing a quantum well structure to meet the V_A , is crucial. To determine the optimum combination of quantum well structure and V_A , we simulated numerous electron trajectories in our MQW under different V_A using a Monte Carlo method (software 'CASINO', available at <http://www.gel.usherbrooke.ca/casino>)²⁰. Figure 4a shows a result for $V_A = 8$ kV.

For more quantitative analyses, Fig. 4b summarizes the V_A dependences of the electron energy absorbed within the quantum well region (left axis) and the ratio of that absorbed energy to the energy irradiated onto the sample (right axis). The former corresponds to the energy used to generate electron-hole pairs in the quantum well region, and was maximized at $V_A = 8$ kV. However,

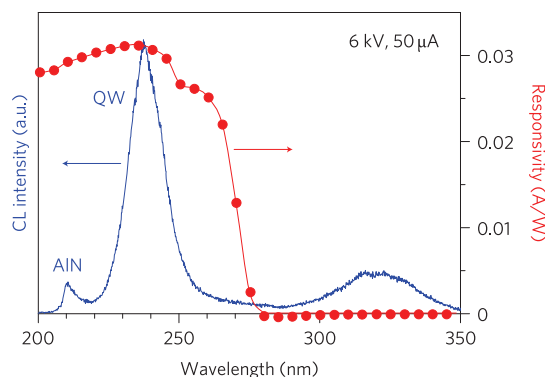


Figure 3 | CL spectrum with photodiode responsivity. CL spectrum of the $\text{Al}_{0.69}\text{Ga}_{0.31}\text{N}/\text{AlN}$ MQW and the responsivity of the $\text{Al}_x\text{Ga}_{1-x}\text{N}$ photodiode measured at room temperature.

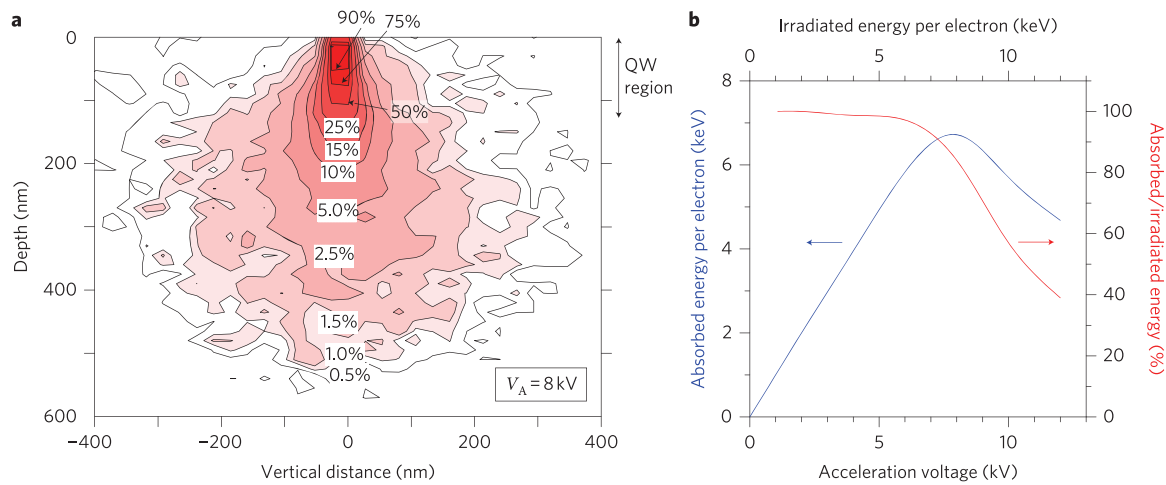


Figure 4 | Electron penetration. **a**, Contour plot of the electron energy for $V_A = 8$ kV simulated by the Monte Carlo method. The assumed structure is an $\text{Al}_{0.69}\text{Ga}_{0.31}\text{N}$ (1 nm)/ AlN (15 nm) eight-period MQW. The vertical axis is the depth from the sample surface. Percentages represent the electron energy with respect to the initial value. For example, ‘90%’ means that 10% of the electron energy is absorbed in the solid. **b**, Summary of the Monte Carlo simulation showing the V_A dependence of the absorbed electron energy within the quantum well region (left axis) and the ratio between absorbed energy and irradiated energy onto the sample (right axis).

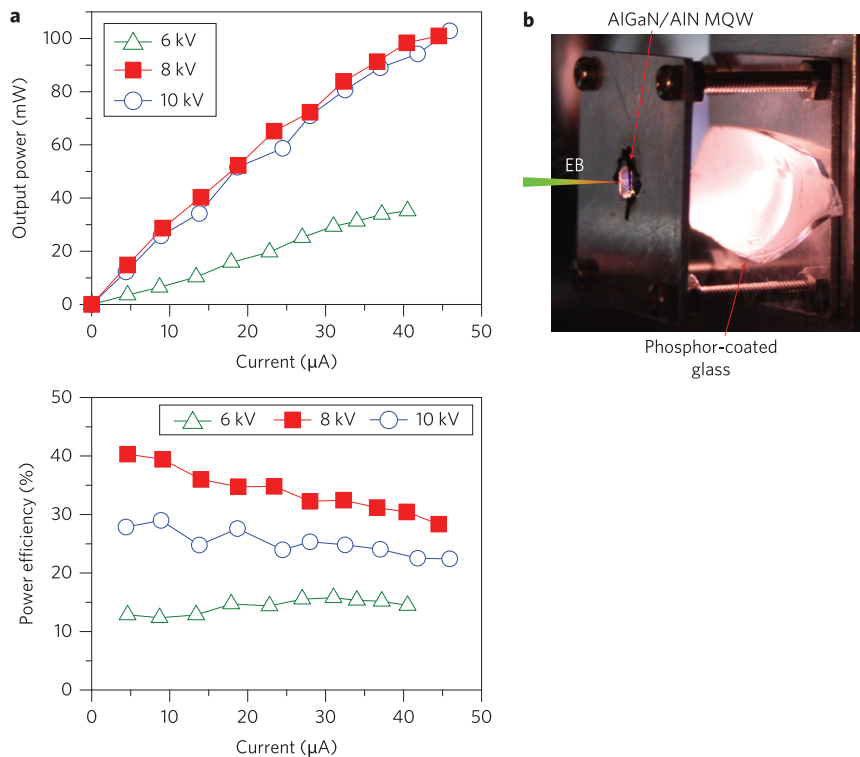


Figure 5 | Electron beam pumping. **a**, P_{out} and PE as functions of irradiated current under different V_A . P_{out} in excess of 100 mW is achieved at $V_A > 8$ kV and $I = 45 \mu\text{A}$. Maximum PE greater than 40% is obtained at $V_A = 8$ kV and $I = 5 \mu\text{A}$. **b**, Photograph showing a phosphor-coated glass excited by UV emission from our $\text{Al}_{0.69}\text{Ga}_{0.31}\text{N}/\text{AlN}$ MQW under 8 kV and 45 μA . All measurements were performed at room temperature.

further increasing V_A decreased it by the mechanism explained above. Therefore, $V_A = 8$ kV should be the best in terms of maximizing P_{out} . On the other hand, the energy ratio (right axis of Fig. 4b) represents the utilization of irradiated electrons within the quantum well region and corresponds to CIE. Again, $V_A > 8$ kV degraded the ratio by the same mechanism. Although the ratio is high for $V_A < 8$ kV, the penetration of electrons is insufficient to cover the entire quantum well region. The simulation therefore indicates that a V_A between 6 and 8 kV is suitable for the current MQW structure.

To confirm the Monte Carlo analysis, P_{out} was experimentally evaluated using the setup shown in Fig. 2. Figure 5a shows P_{out} and PE as a function of irradiated current (I). P_{out} exceeded 100 mW with $V_A = 8$ kV and $I = 45 \mu\text{A}$. However, further increasing V_A did not increase P_{out} , which is consistent with the simulation (Fig. 4b). Furthermore, the PE was also the highest with $V_A = 8$ kV, and was more than 40% for $I = 5 \mu\text{A}$. These experimental results indicated that $V_A = 8$ kV is the most suitable V_A for our MQW. It is noteworthy that the achieved P_{out} of 100 mW and PE of 40% are about two orders of magnitude higher than the values reported

for LEDs emitting at 250 nm (ref. 12) and EB pumped nitride semiconductors^{17,18}. One discrepancy with the simulation was that $V_A = 6$ kV did not provide a PE comparable to that for $V_A = 8$ kV. A possible reason is the carrier density dependent IQE (unpublished data). Also, the mechanism for the PE drop observed for larger currents has yet to be clarified. These are to be the subjects of future studies.

The efficiencies are discussed, using experimental results of IQE = 57%, an emission energy (E) of 5.2 eV (238 nm), and P_{out} of 100 mW for $V_A = 8$ kV and $I = 45$ μ A. As detailed in the Methods, we consider the relationship $PE/\eta_{\text{EH}} = \text{IQE} \times \text{LEE} \times \text{CIE}$, where η_{EH} ($0 \leq \eta_{\text{EH}} \leq 1$) is the yield for an irradiated electron to generate electron-hole pairs in solids. It is difficult to experimentally quantify CIE. Therefore, the value estimated using the Monte Carlo simulation (right axis of Fig. 4b) was used, in other words, 84% for $V_A = 8$ kV. Substituting these quantities into $PE/\eta_{\text{EH}} = \text{IQE} \times \text{LEE} \times \text{CIE}$ results in $\eta_{\text{EH}} \times \text{LEE} = 0.58$. For example, LEE = 58% for $\eta_{\text{EH}} = 100\%$. Although in order to determine these values we have to determine one of them in other experiments, the condition $\eta_{\text{EH}} \times \text{LEE} = 0.58$ seems reasonable, because the emitted light is efficiently extracted from the roughened back of the sapphire substrate.

Figure 5b shows a photograph of a phosphor-coated glass excited by UV emission from our $\text{Al}_{0.69}\text{Ga}_{0.31}\text{N}/\text{AlN}$ MQW under the conditions of 8 kV and 45 μ A. The coated phosphors were identical to those used for fluorescent lamps. In this particular case, the distance between the MQW and the target phosphors was ~ 15 mm, which is much larger than that between the MQW and photodiode used for Fig. 5a (3 mm). Nevertheless, the phosphors emitted a dazzling white colour, confirming the high P_{out} from our MQW.

The present results suggest that the low EQEs of state-of-the-art UV LEDs are not due to low IQEs, but predominantly to low CIEs. However, for EB pumped devices, once high-quality quantum wells have been obtained, significant levels of PE are expected. It should be emphasized that the EB operating conditions in this study (~ 8 kV and < 50 μ A) are accessible using portable field-emission devices. Additionally, preliminary experiments showed that P_{out} did not decrease at all over a period of about an hour with $V_A = 6$ kV and $I = 35$ μ A. We therefore believe that EB pumping of quantum wells is extremely effective for generating UV light, and the present developments form a significant step towards a next-generation, compact, high-efficiency UV light source.

Methods

Estimation of IQE. A widely used method with which to experimentally estimate IQE is described. The ratio of the PL integrated intensity at room temperature to that at a low temperature is first evaluated. With an assumption that non-radiative recombination processes can be neglected at low temperatures²¹, the PL intensity at low temperatures can be regarded as an IQE of 100%. The abovementioned PL intensity ratio can then be used to estimate the IQE at room temperature.

Crystal growth. The growth method was modified migration-enhanced epitaxy (MEE) based on metallorganic vapour phase epitaxy⁶⁻⁸. This method is a hybrid of conventional MEE and a simultaneous source supply, where the latter is inserted into the former. High-quality AlN with a thickness of ~ 600 nm was initially grown on a sapphire (0001) substrate at 1,200 °C by modified MEE using trimethylaluminium (TMA) and ammonia as source precursors. $\text{Al}_x\text{Ga}_{1-x}\text{N}/\text{AlN}$ MQWs were then fabricated by modified MEE while supplying additional trimethylgallium (TMG) together with the TMA. As well as controlling the thickness of the barrier and well layers on a per-growth-cycle basis (AlN barriers, 21 cycles; AlGaN wells, 1 cycle), this method enabled an atomically flat surface to be maintained. To induce gallium into the quantum wells, the growth temperature was decreased from 1,200 to 1,080 °C. The quantum well parameters, including aluminium composition, well widths and barrier widths, were derived from transmission electron microscopy and the satellite peaks observed in X-ray diffraction (XRD) measurements. Reciprocal space mapping by XRD was also performed to confirm the coherent growth of $\text{Al}_x\text{Ga}_{1-x}\text{N}/\text{AlN}$ MQWs with respect to AlN underlying layers.

Optical measurements. The PL measurements were carried out at 8.5 K and room temperature. The excitation source was a pulsed ArF excimer laser ($\lambda = 193$ nm, $\tau = 4$ ns, 25 Hz and 100 kW cm⁻²). The spectra were acquired using a 30-cm

monochromator (resolution, 0.1 nm) in conjunction with a liquid-nitrogen-cooled charge-coupled device camera.

Figure 2 shows the setup for the CL measurements. The sample, EB gun and photodiode were loaded in the same vacuum chamber. EB generated by thermionic emission was accelerated by V_A and focused using electromagnetic lenses. The V_A varied between 0.1 and 30 kV, and the emission current was varied below 110 μ A. The irradiated current was estimated using a Faraday cup adjacent to the sample. The $\text{Al}_x\text{Ga}_{1-x}\text{N}$ photodiode was produced by ALGAN K.K., Japan, and its responsivity (shown in Fig. 3) was calibrated at the National Metrology Institute of Japan²². Both the sample and the photodiode were mounted on an aluminium block, which served as a heat sink, so that the effects of heat generation by non-radiative processes could be neglected. The luminescence excited by EB (that is, CL) was collected outside the vacuum chamber that held the sample through a viewing window composed of synthetic quartz. The spectra were acquired by the same detecting equipments for the PL measurements.

Definitions of efficiencies for EB pumping. To estimate EQE during EB pumping, it should be noted that one irradiated electron generates multiple electron-hole pairs in solids. Using the yield (η_{EH}) of that process, the number of electron-hole pairs per irradiated electron is expressed by $\eta_{\text{EH}}V_A/E$ ($0 \leq \eta_{\text{EH}} \leq 1$), which leads to the EQE definition of $(P_{\text{out}}/eE)/((\eta_{\text{EH}}V_A/E)(I/e))$. Here, e is the elementary charge. Then, taking $PE = P_{\text{out}}/(IV_A)$ and $\text{EQE} = \text{IQE} \times \text{LEE} \times \text{CIE}$ into account, we obtain $PE/\eta_{\text{EH}} = \text{IQE} \times \text{LEE} \times \text{CIE}$.

Received 3 June 2010; accepted 18 August 2010;

published online 26 September 2010

References

1. Taniyasu, Y., Kasu, M. & Makimoto, T. An aluminium nitride light-emitting diode with a wavelength of 210 nanometres. *Nature* **441**, 325–328 (2006).
2. Khan, A., Balakrishnan, K. & Katona, T. Ultraviolet light-emitting diodes based on group three nitrides. *Nature Photon.* **2**, 77–84 (2008).
3. Li, J., Nam, B., Nakarmi, M. L., Lin, J. Y. & Jiang, H. X. Band structure and fundamental optical transitions in wurtzite AlN. *Appl. Phys. Lett.* **83**, 5163–5165 (2003).
4. Shatalov, M. *et al.* Efficiency of light emission in high aluminum content AlGaN quantum wells. *J. Appl. Phys.* **105**, 073103 (2009).
5. Bhattacharyya, A., Moustakas, T. D., Zhou, L., Smith, D. J. & Hug, W. Deep ultraviolet emitting AlGaIn quantum wells with high internal quantum efficiency. *Appl. Phys. Lett.* **94**, 181907 (2009).
6. Banal, R. G., Funato, M. & Kawakami, Y. Initial nucleation of AlN grown directly on sapphire substrates by metalorganic vapor phase epitaxy. *Appl. Phys. Lett.* **92**, 241905 (2008).
7. Banal, R. G., Funato, M. & Kawakami, Y. Growth characteristics of AlN on sapphire substrates by modified migration enhanced epitaxy. *J. Cryst. Growth* **311**, 2834–2836 (2009).
8. Banal, R. G., Funato, M. & Kawakami, Y. Characteristic of high Al-content AlGaIn/AlN quantum wells fabricated by modified migration enhanced epitaxy. *Phys. Status Solidi c* **7**, 2111–2114 (2010).
9. Banal, R. G., Funato, M. & Kawakami, Y. Optical anisotropy in [0001]-oriented $\text{Al}_x\text{Ga}_{1-x}\text{N}/\text{AlN}$ quantum wells ($x > 0.69$). *Phys. Rev. B* **79**, 121308(R) (2009).
10. Fujioka, A., Misaki, T., Murayama, T., Narukawa, Y. & Mukai, T. Improvement in output power of 280-nm-deep ultraviolet light-emitting diode by using AlGaIn multi quantum wells. *Appl. Phys. Express* **3**, 041001 (2010).
11. Pernot, C. *et al.* Improved efficiency of 255–280 nm AlGaIn-based light-emitting diodes. *Appl. Phys. Express* **3**, 061004 (2010).
12. Hirayama, H. *et al.* 222–282 nm AlGaIn and InAlGaIn-based deep-UV LEDs fabricated on high-quality AlN on sapphire. *Phys. Status Solidi a* **206**, 1176–1182 (2009).
13. Hirayama, H., Tsukada, Y., Maeda, T. & Kamata, N. Marked enhancement in the efficiency of deep-ultraviolet AlGaIn light-emitting diodes by using a multi quantum-barrier electron blocking layer. *Appl. Phys. Express* **3**, 031002 (2010).
14. Narukawa, Y. *et al.* Ultra-high efficiency white light emitting diodes. *Jpn J. Appl. Phys.* **45**, L1084–L1086 (2006).
15. Yamada, M. *et al.* InGaIn-based near-ultraviolet and blue-light-emitting diodes with high external quantum efficiency using a patterned sapphire substrate and a mesh electrode. *Jpn J. Appl. Phys.* **41**, L1431–L1433 (2002).
16. Madelung, O. *Semiconductors: Data Handbook* 3rd edn, Ch. 2 (Springer, 2003).
17. Watanabe, K., Taniguchi, T., Niiyama, T., Miya, K. & Taniguchi, M. Far-ultraviolet plane-emission handheld device based on hexagonal boron nitride. *Nature Photon.* **3**, 591–594 (2009).
18. Miyake, H. *et al.* Fabrication of deep-ultraviolet light source using AlGaIn on AlN/sapphire. *8th International Symposium on Semiconductor Light Emitting Devices (ISSLED)*, E2 (Beijing, 2010).
19. Göbel, E. O., Jung, H., Kuhl, J. & Ploog, K. Recombination enhancement due to carrier localization in quantum well structures. *Phys. Rev. Lett.* **51**, 1588–1591 (1983).
20. Drouin, D. *et al.* CASINO V2.42—a fast and easy-to-use modeling tool for scanning electron microscopy. *Scanning* **29**, 92–101 (2007).

21. Miller, R. C., Kleinman, D. A., Nordland, W. A. Jr & Gossard, A. C. Luminescence studies of optically pumped quantum wells in GaAs–Al_xGa_{1-x}As multilayer structures. *Phys. Rev. B* **22**, 863–871 (1980).
22. Saito, T. *et al.* UV/VUV photodetectors using group III-nitride semiconductors. *Phys. Status Solidi c* **6**, S658–S661 (2009).

Acknowledgements

The authors would like to thank T. Hitora (president CEO, AlGaIn K.K., Japan) for his support regarding the AlGaIn photodiodes. This work was partly supported by a Grant-in-Aid for Scientific Research (18069007) and the Global Center-of-Excellence (G-COE) Programme of the Ministry of Education, Culture, Sports, Science and Technology of Japan.

Author contributions

Y.K. supervised the project. R.G.B. performed crystal growth and PL measurements. Y.K, M.F., T.O. and K.K. conceived and designed the CL experiments. T.O. and K.K. performed the experiments, and T.O. carried out the simulation. All authors participated in the analyses, discussions of the data and writing the paper.

Additional information

The authors declare no competing financial interests. Reprints and permission information is available online at <http://npg.nature.com/reprintsandpermissions/>. Correspondence and requests for materials should be addressed to Y.K.